

Effect of Temperature on the Structural and Magnetic Properties of $\text{Ni}_x\text{Co}_{1-x}\text{Fe}_2\text{O}_4$ Nanoparticles

V.S. Bushkova*

Vasyl Stefanyk Pre-Carpathian National University, 57, Shevchenko St., 76025 Ivano-Frankivsk, Ukraine

(Received 28 December 2015; published online 15 March 2016)

In the work, single-phase ferrite powders of $\text{Ni}_x\text{Co}_{1-x}\text{Fe}_2\text{O}_4$ systems were synthesised using the sol-gel technology with participation of auto-combustion. It was found that the average size of coherent scattering regions does not exceed 62 nm. The dependences of the lattice parameter, X-ray density and specific surface area of the ferrite powders versus the nickel content were obtained. The unit cell parameter a decreases linearly with nickel concentration due to smaller ionic radius of nickel. After annealing of ferrite powders at the temperature of 1300 °C, which were pressed in the form of a toroid at the pressure of $3.3 \cdot 10^8$ Pa, X-ray analysis showed that the found rings are single-phase with the cubic structure of spinel space group $Fd\bar{3}m$. The dependence of the initial permeability on the degree of substitution of cobalt cations by nickel cations is obtained. It is revealed that the crystallite size has a significant influence on the magnetic properties of the samples. With decreasing crystallite size of nickel-cobalt ferrite, the Curie temperature decreases. Because of strengthening of the A - B exchange interaction, the increase in the Curie temperature occurs with increasing parameter x . It is shown that the smaller the particle size, the greater the thickness of the surface layer with significant violations of the magnetic structure.

Keywords: Sol-gel technology, Nickel-cobalt ferrite, Lattice parameter, Specific surface area, Initial permeability, Curie temperature.

DOI: [10.21272/jnep.8\(1\).01002](https://doi.org/10.21272/jnep.8(1).01002)

PACS numbers: 75.50.Tt, 81.07.Wx, 81.20.Fw, 75.30.Kz

1. INTRODUCTION

Ferrite nanoparticles, for today, are of great interest in the scientific aspect. Nanoferrites are promising materials due to a wide spectrum of applications in modern science and technology [1]. Recently, they have attracted considerable attention of researchers because of their structural, magnetic and electrical properties [2]. Moreover, their magnetic properties can be controlled taking into account the practical application by the right choice of several bivalent cations and their correlations in the structure of ferrites.

Nanoscale powders have opened a new direction in physical material science, and the need for materials with high specific resistance has led to the synthesis of ferrites of different composition.

Macro-crystalline cobalt ferrite is known as a hard-magnetic material with high coercivity and low magnetization. These properties, together with high physical and chemical stability, promote its use in data storage devices as well as in magneto-optical and magneto-electric devices [3-6]. In contrast to CoFe_2O_4 , nickel ferrite is a typical soft magnetic material, which has many applications in electronic devices, namely, high-frequency inductance coils, transformers, antennas, etc. [7-9].

Both the magnetic and electrical properties of ferrites certainly depend not only on their chemical composition, but also on the synthesis method. This work is devoted to the study of $\text{Ni}_x\text{Co}_{1-x}\text{Fe}_2\text{O}_4$ ferrite nanopowders obtained by the sol-gel method with participation of auto-combustion (SGA).

2. EXPERIMENTAL

Ferrites of $\text{Ni}_x\text{Co}_{1-x}\text{Fe}_2\text{O}_4$ system ($x = 0.0, 0.1, 0.2, 0.3, 0.4, 0.5$) were synthesized by the SGA method [10].

The phase composition was controlled using the X-ray analysis, which was performed by the diffractometer DRON-3 with $\text{Cu}(K\alpha)$ -radiation in the range of scan angles of $20^\circ \leq 2\theta \leq 60^\circ$ with the step of 0.02° .

The determination of the structural-adsorption characteristics of the nickel-cobalt powders was carried out by the analysis of the sorption isotherms of nitrogen at the temperature of 77 K on the automated sorptometer Quantachrome Autosorb (Nova 2200e). The specific surface area of the powders was calculated using the multi-point Brunauer-Emmett-Teller (BET) method [11] for the linear dependence of $1/[W(P_0/P) - 1]$ on P/P_0 in the region of adsorption isotherm restricted by the range of $P/P_0 = 0.05-0.35$.

Ferrite cores in the form of a toroid are obtained by pressing under a pressure of $3.3 \cdot 10^8$ Pa of synthesized powders with the outer (2.3 cm) and inner (1.4 cm) diameters and height of about 0.2 cm. These samples were sintered at the temperature of 1300 °C during 5 hours in the atmosphere of air with a gradual cooling.

In order to determine the initial magnetic permeability, the coils were produced by the deposition of a winding of thin copper wire on the ferrite rings. For the analysis of the temperature dependence of the initial magnetic permeability of ferrites of the $\text{Ni}_x\text{Co}_{1-x}\text{Fe}_2\text{O}_4$ composition, we have performed measurements of the inductance of coils with a ferrite core at the frequency of 1 kHz using the digital meter LCR of the type E7-8 in a weak magnetic field ($H \rightarrow 0$).

3. RESULTS AND DISCUSSION

3.1 X-ray studies of the synthesized powders

In Fig. 1 we illustrate the X-ray diffraction patterns of the nickel-cobalt ferrite powders obtained after auto-

* bushkovavira@gmail.com

combustion. According to the performed analysis, peaks of the diffractograms indicate the presence of the cubic structure of spinel space group $Fd\bar{3}m$.

The average sizes of the coherent scattering regions (CSR) of the Ni-Co ferrite powders calculated using the Scherrer formula, lattice parameter a , and X-ray density d_x are represented in Table 1.

The decrease in the lattice parameter with increasing number of Ni^{2+} cations in the structure of nickel-cobalt ferrites can be explained based on the difference in ionic radiuses. In the studied $Ni_xCo_{1-x}Fe_2O_4$ system, larger Co^{2+} ions are substituted by smaller Ni^{2+} ions, therefore the lattice parameter decreases in this case. As for the X-ray density, its value linearly increases with nickel concentration, since Ni atom is heavier than the Co one.

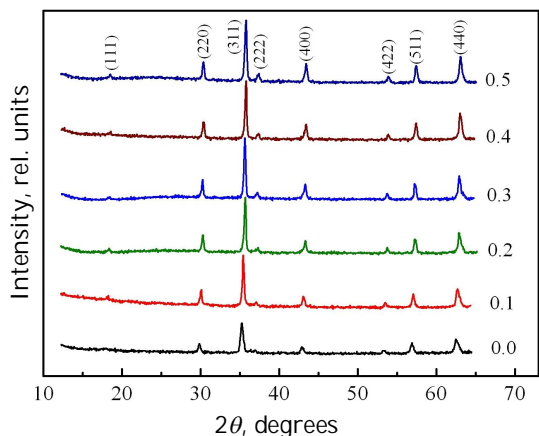


Fig. 1 – Diffraction patterns of the nickel-cobalt powders

Table 1 – Structural parameters of the SGA ferrite powders

The degree of substitution, x	$\langle D \rangle$, nm	a , nm	d_x , g/cm ³
0.0	39	0.8381	5.293
0.1	52	0.8375	5.303
0.2	57	0.8368	5.316
0.3	63	0.8364	5.324
0.4	59	0.8358	5.335
0.5	57	0.8353	5.343

3.2 Adsorption characteristic of ferrite powders

The values of the specific surface area of the studied system of ferrites are calculated by the experimentally obtained adsorption isotherms of nitrogen using multi-point BET method. The values of the specific surface area of ferrite powders are represented in Table 2. The $CoFe_2O_4$ powder has, as expected, the greatest surface area. We should note that specific surface area of the powders decreases with addition of Ni^{2+} cations in Ni-Co ferrites to $x=0.3$, probably due to the increase in the CSR sizes, and increases because of their decrease.

Using the BET theory, the crystallite size d_{BET} was evaluated as follows

$$d_{BET} = \frac{6}{\rho S_{num}},$$

where ρ is measured in kg/m³, S_{num} – in m²/kg, and d_{av} – in m. Or

$$d_{BET} = \frac{6 \cdot 10^3}{\rho S_{num}},$$

where ρ is the density, S_{num} is the specific surface area.

The calculated values of d_{BET} by the above relation are given in Table 2.

Comparing the average sizes of particles calculated by the Scherrer formula and formula (7), we can assume that the obtained values of d_{BET} are the average sizes of agglomerates of ferrite powders.

Table 2 – Dependence of the specific surface area and average size of agglomerates on the parameter x of nickel-cobalt ferrite powders

The degree of substitution, x	S_{num} , m ² /g	d_{BET} , nm
0.0	14.1	80
0.1	10.2	111
0.2	8.8	128
0.3	7.6	148
0.4	8.5	132
0.5	9.7	116

3.3 X-ray studies of nickel-cobalt ferrite rings

In Fig. 2 we present the X-ray diffraction patterns of the ferrite rings of the $Ni_xCo_{1-x}Fe_2O_4$ system. Both for the ferrite powders and their rings sintered at the temperature of 1300 °C during 5 hours, peaks of the diffractograms imply the presence of the cubic structure of spinel space group $Fd\bar{3}m$. This indicates that spinel does not decompose to the corresponding oxides at this temperature.

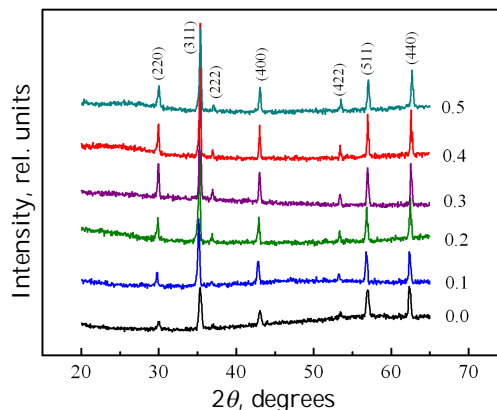


Fig. 2 – Diffraction patterns of the nickel-cobalt rings

In Fig. 3 we illustrate the dependence of the average CSR sizes of SGA powders and sintered rings on the content of Ni^{2+} cations in the composition of the studied ferrites. The calculation results showed that the average CSR size of ferrite rings is in the range of 42-94 nm.

For the ferrite rings, the values of the lattice parameter a and X-ray density d_x are obtained by the following formulas:

$$a = \frac{\lambda}{2 \sin \theta} \sqrt{h^2 + k^2 + l^2},$$

where l is the X-ray radiation wavelength; θ are the an-

gles, on which the peaks were observed; h, k, l are the Miller indices;

$$d_x = \frac{8M}{N_A a^3},$$

where M is the molar mass of $Ni_xCo_{1-x}Fe_2O_4$ ferrites, N_A is the Avogadro number, and are shown in Fig. 4.

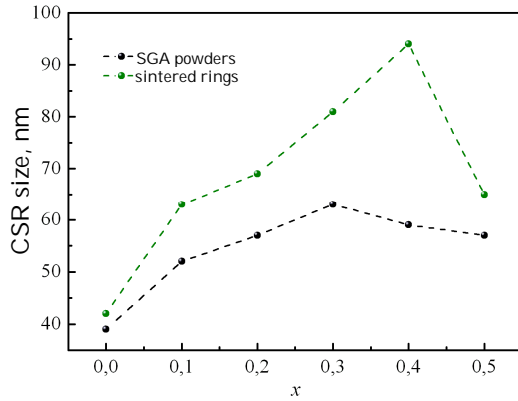


Fig. 3 – Dependence of the CSR size on the composition x

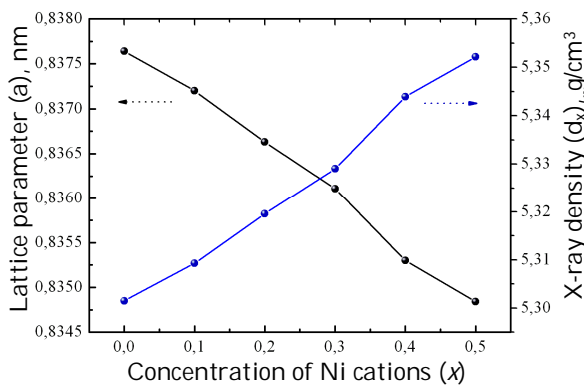


Fig. 4 – Dependence of the lattice parameter and density d_x of the rings on Ni^{2+}

As seen from Fig. 4, with increasing content of Ni^{2+} cations, the lattice parameter of the rings decreases and the X-ray density increases in the $Ni_xCo_{1-x}Fe_2O_4$ system. We should note that lattice parameter of the rings for each composition of the studied ferrites is slightly less than its value for the synthesized SGA powders. The value of the X-ray density of the rings similarly increases compared with the ferrite powders. Obviously, these changes are associated with the increase in the crystallites size in the rings occurred as a result of prolonged sintering.

The authors of [22] investigating the influence of the particles size on the properties of the $CoFe_2O_4$ powder have revealed that for the particles of the size of 6 nm, the lattice parameter is equal to 0.8177 nm. In turn, for the particles with the size of 50 nm obtained during the additional sintering at the temperature of 900 °C, the above mentioned parameter is 0.8379 nm, which is very close to the value of $a = 0.8376$ nm calculated for the ferrite ring of the same composition with the average CSR size of 42 nm.

Porosity P of the samples in the form of a toroid (see Table 3) is calculated by the formula

$$P = 1 - \frac{d_m}{d_x},$$

where d_m is the volume density.

The table data implies that the ring of the $CoFe_2O_4$ composition, whose volume density is minimal, has the highest porosity, and the ring of the $Ni_{0.4}Co_{0.6}Fe_2O_4$ composition with the maximum value of d_m has the lowest one. We should note that there is a clear correlation between the CSR sizes of the rings and their volume density.

Table 3 – Dependence of the volume density and porosity of the rings on the parameter x

The degree of substitution, x	d_m , g/cm ³	P , %
0.0	4.18	21.1
0.1	4.25	19.9
0.2	4.41	17.1
0.3	4.49	15.7
0.4	4.57	14.4
0.5	4.56	14.8

3.4 Temperature dependence of the initial magnetic permeability of ferrite rings

The initial magnetic permeability μ_i is an important magnetic characteristic of materials. As a rule, the value of μ_i depends on two factors [13], namely, the contribution of spin rotation and contribution of domain wall displacement. However, the contribution of spin rotation is much less than the contribution of domain wall displacement [14], therefore, the initial magnetic permeability is usually described by the expression

$$\mu_i - 1 = \frac{3\pi M_S^2 D}{4\gamma},$$

where M_S is the saturation magnetization, D is the average grain size, γ is the domain wall energy proportional to the crystallographic anisotropy constant K_1 [15, 16].

It is known that saturation magnetization and anisotropy constant decrease with increasing temperature. Together with this, K_1 decays faster than M_S . The initial magnetic permeability will take the maximum value at $K_1 \rightarrow 0$ [17] according to the expression

$$\mu_i \approx \frac{M_S^2 D}{\sqrt{K_1}}.$$

Thus, according to the equation (12), μ_i is directly proportional to M_S and inversely proportional to K_1 .

In Fig. 5 we illustrate the temperature dependence of the initial magnetic permeability of ferrites of the $Ni_xCo_{1-x}Fe_2O_4$ system. As seen from Fig. 5, at a certain temperature for each composition of the studied system the magnetic permeability reaches its maximum value, after that it sharply decreases. The same phenomenon has been already observed in Li-Cu [18], Cu-Zn [19], Mg-Cu-Zn [20] and other ferrites. We should note that this behavior of the dependence $\mu_i(T)$, according to the Globus model, indicates high uniformity of all the samples [21]. Proceeding from this, $Ni_{0.3}Co_{0.7}Fe_2O_4$ sample is the most uniform one.

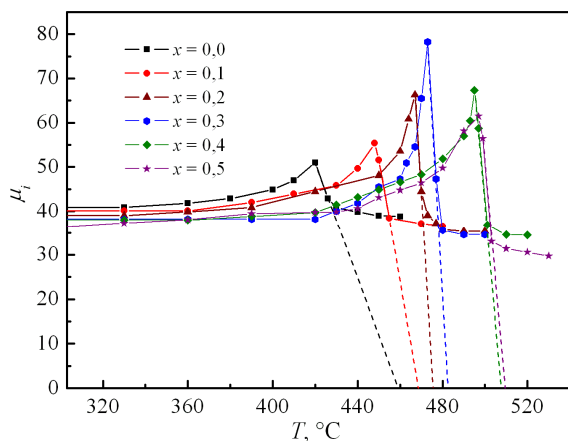


Fig. 5 – Temperature dependence of the magnetic permeability of nickel-cobalt ferrites

It is known [22] that for the initial magnetic permeability one can observe the maximum at a temperature, which is slightly lower than the Curie point. Therefore, a linear extrapolation of the sharpest region of the dependence $\mu_i(T)$ to the intersection with the abscissa axis was carried out for the determination of the real Curie temperature of ferrites.

Such behavior of the temperature dependence of the initial magnetic permeability can be explained by the increase in the domain wall mobility with increasing temperature that promotes the growth of magnetization. However, the intensification process of the domain wall motion cannot proceed infinitely. So, after reaching the Curie temperature, thermal motion becomes so intense that its energy is sufficient for the destruction of domains. This means that the substance loses its ferromagnetic properties and passes into the paramagnetic state.

On the other hand, increase in μ_i with increasing temperature is explained by the decrease in the magnetostriction and magnetic crystallographic anisotropy constants, i.e. the forces which counteract the domain wall displacement and rotation of domain magnetic moments are attenuated when heating a ferromagnet. High-temperature decay of the magnetic permeability at a temperature of $T > T_{\max}$ is associated with a sharp decrease in the domain magnetization.

In Table 4 we present the values of the Curie temperature and magnetic permeability (at room temperature) for all the samples. Analyzing the table data, we should note that μ_i decays and T_c increases with increasing degree of substitution.

Curie temperature is determined by the strongest exchange interaction, i.e. the superexchange A - B interaction. It was established in [23] that substitution in the

Table 4 – Dependence of the initial magnetic permeability and Curie temperature on the degree of substitution x

The degree of substitution, x	μ_i	$T_c, ^\circ\text{C}$
0.0	38.8	459
0.1	37.1	468
0.2	35.4	476
0.3	34.6	483
0.4	34.5	507
0.5	33.1	509

$\text{Ni}_x\text{Co}_{1-x}\text{Fe}_2\text{O}_4$ system of Co^{2+} cations by Ni^{2+} cations leads to the strengthening of the superexchange A - B interaction that is expressed in a monotonic increase in the Curie temperature. At the same time, increase in the exchange interaction between A and B cations of spinel sublattices with increasing parameter x leads to the increase in the crystallographic anisotropy and magnetostriction constants. Due to this fact, the initial magnetic permeability decays, as a rule, in weak fields.

As known from [24], for the macrocrystalline CoFe_2O_4 ferrite obtained using the ceramic technology, the Curie temperature is approximately equal to 520 °C. However, based on the data of Table 4, T_c for a sample of the same composition is much lower than the above mentioned temperature. Moreover, the same trend also persists for other samples of the $\text{Ni}_x\text{Co}_{1-x}\text{Fe}_2\text{O}_4$ system. Decrease in the Curie temperature compared with the macrocrystalline samples can be associated with the increase in the distance between the magnetic moments of the A and B sublattices of the studied system that is confirmed by the increase in the lattice parameter a .

Moreover, it is known that the smaller the grain size, the more noticeable is the influence of different factors on the state of surface layers and, correspondingly, on the sample properties in whole. Obviously, the greater part of atoms in the composition of these fine particles belongs to the surface layer, the more exchange bonds between atoms are found to be dangling. Therefore, according to the Curie point, there is a possibility to obtain the quantitative information about the structural features of the surface layer of a nanoparticle.

Considering that the particles are spherical with the same radius r , we assume that a half of the exchange bonds, due to which there is a magnetic ordering inside the particle below its Curie point, of the surface magneto-active atoms will be dangling. In the case of a macrocrystalline particle, the number of exchange bonds per unit volume is equal to n , then for the surface magneto-active atoms of the nanoparticle this number will be $n/2$. Considering that Curie temperature for the nanoparticle is proportional to the average number of exchange bonds, the ratio of the Curie temperatures of nano- and macrocrystalline particle can be expressed by the formula

$$\frac{T_c'}{T_c} = 1 - \frac{3\Delta r}{2r},$$

where Δr is the thickness of the layer with half dangling exchange bonds. In this case, Δr is the averaged parameter, which characterizes the features of the defect structure of nanoparticles. That is, the smaller the particles sizes, the greater effective thickness Δr of the violation of their magnetic structure. As follows from (13), parameter $\Delta r \rightarrow 0$ at $T_c' \rightarrow T_c$.

In the study of nickel-cobalt ferrites synthesized using the mechanical-chemical process, the authors of [25] obtained for the cobalt ferrite with the crystallite size of about 200 nm the values of the Curie temperature equal to 516 °C, while for the ferrite of the same chemical composition obtained by the ceramic technology $T_c = 520$ °C. Having performed simple calculations, we determined the imperfection parameter for the CoFe_2O_4 ferrite with the size of 200 nm which is equal to 0.51 nm. Based on similar considerations, for the studied ring at $x = 0.0$

($\langle D \rangle = 42$ nm) we obtained $\Delta r = 1.64$ nm. Obviously, the obtained values of the Curie temperature for ferrites of the $\text{Ni}_x\text{Co}_{1-x}\text{Fe}_2\text{O}_4$ system can be explained by the manifestation of the size effects.

This is confirmed by experimentally obtained close values of the Curie temperature for the samples with $x = 0.4$, $x = 0.5$. It is clearly seen from Fig. 3 that particles size of the sintered $\text{Ni}_{0.4}\text{Co}_{0.6}\text{Fe}_2\text{O}_4$ sample is much larger than the particles of $\text{Ni}_{0.5}\text{Co}_{0.5}\text{Fe}_2\text{O}_4$. Because of this fact, Curie temperature of the $\text{Ni}_{0.4}\text{Co}_{0.6}\text{Fe}_2\text{O}_4$ ring declines towards higher temperatures with respect to the linear dependence $T_c(x)$.

4. CONCLUSIONS

Thus, the SGA method allowed to synthesize single phase nanopowders of nickel-cobalt ferrites. The average CSR size of ferrite powders with the spinel structure is in the range of 39-62 nm, while the crystallite size of the rings does not exceed 94 nm. It is established that the average sizes of powder agglomerates belong to the range of 80-148 nm.

The lattice parameter and X-ray density are calculated for both the SGA powders and ferrites sintered at

the temperature of 1300 °C. It is found that parameter a decreases, while X-ray density linearly increases with increasing concentration of Ni^{2+} cations for two systems of nickel-cobalt ferrites.

It should be noted that there is a clear correlation between the CSR sizes of the rings and their volume density. Toroid of the $\text{Ni}_{0.4}\text{Co}_{0.6}\text{Fe}_2\text{O}_4$ composition with the maximum CSR value, namely, 94 nm, was found to be the sample, whose porosity is the lowest.

The initial magnetic permeability and Curie temperature are determined for each composition of the studied system. With increasing number of nickel cations in the composition of the $\text{Ni}_x\text{Co}_{1-x}\text{Fe}_2\text{O}_4$ system, there is a decay of the magnetic permeability, at that the value of T_c increases. Increase in the Curie temperature with increasing parameter x occurs due to the strengthening of the superexchange A - B interaction, since Ni^{2+} cations occupy exclusively B sublattice displacing in this case Fe^{3+} cations to A sublattice.

The obtained values of the Curie temperature compared with its values for bulk samples indicate a significant impact of the surface layer thickness of crystallites with magnetic structural imperfection on the properties of ferrite rings that is associated with the size effects.

REFERENCES

- Q. Song, Z.J. Zhang, *J. Am. Chem. Soc.* **126**, 6164 (2004).
- Y.H. Hou, Y.J. Zhao, Z.W. Liu, H.Y. Yu, X.C. Zhong, W.Q. Qiu, D.C. Zeng, L.S. Wen, *J. Phys. D: Appl. Phys.* **43**, 445003 (2010).
- J. Ding, Y.J. Chen, Y. Shi, S. Wang, *Appl. Phys. Lett.* **77**, 3621 (2000).
- Y. Suzuki, R.B. van Dover, E.M. Gyorgy, J.M. Philips, V. Korenivski, D.J. Werder, C.H. Chen, R.J. Cava, J.J. Krajewski, W.F. Peck, K.B. Do, *Appl. Phys. Lett.* **68**, 714 (1996).
- J. Ding, T. Reynold, W.F. Miao, P.G. McCormick, R. Street, *Appl. Phys. Lett.* **65**, 7074 (1994).
- B. Zhou, Y.W. Zhang, Y.J. Yu, C.S. Liao, C.H. Yan, L.Y. Chen, S.Y. Wang, *Phys. Rev. B* **68**, 24426 (2003).
- Y. Qu, H. Yang, N. Yang, Y. Fan, H. Zhu, G. Zou, *Mater. Lett.* **60**, 3548 (2006).
- M.H. Sousa, F.A. Tourinho, *J. Phys. Chem. B* **105**, 1168 (2001).
- F. Mazaleyrat, L.K. Varga, *J. Magn. Magn. Mater.* **215**, 253 (2000).
- V.S. Bushkova, *Int. J. Chem., Nucl., Mater. Metallurg. Eng.* **9**, 357 (2015).
- S. Brunauer, P.H. Emmett, E. Teller, *J. Am. Chem. Soc.* **60**, 309 (1938).
- K. Vasundhara, S.N. Achary, S.K. Deshpande, P.D. Babu, S.S. Meena, et al., *J. Appl. Phys.* **113**, 194101 (2013).
- O.F. Caltun, L. Spinub, A.L. Stancua, L.D. Thungb, W. Zhou, *J. Magn. Magn. Mater.* **242**, 160 (2002).
- G. Baca, R. Valenzuela, M.A. Escobar, L.F. Magaña, *J. Appl. Phys.* **57**, 4183 (1985).
- T.Y. Byun, S.C. Bycon, K.S. Hong, *IEEE T. Magn.* **35**, 3445 (1999).
- M. Guyot, A. Globus, *phys. status solidi b* **52**, 427 (1972).
- J. Loaec, *J. Phys. D: Appl. Phys.* **26**, 963 (1993).
- S.M. Hoque, M.S. Ullah, F.A. Khan, M.A. Hakim, D.K. Saha, *Physica B: Condens. Matt.* **406**, 1799 (2011).
- A.A. Sattar, M.A. Samy, *J. Mater. Sci.* **37**, 4499 (2002).
- M.M. Haque, M. Huq, M.A. Hakim, *J. Magn. Magn. Mater.* **320**, 2792 (2008).
- A. Globus, H. Pascard, V.J. Cagan, *J. Physique* **38**, I (1977).
- F. Nesa, A.K.M. Zakaria, M.A. Saeed Khan, S.M. Yunus, A.K. Das, S.-G. Eriksson, M.N.I. Khan, D.K. Saha, M.A. Hakim, *World J. Condens. Matt. Phys.* **2** No 1, 27 (2012).
- V.S. Bushkova, *J. Nano-Electron. Phys.* **7** No 3, 03021 (2015).
- S. Krupichka, *Fizika ferritov i rodstvennykh im materialov* (Moskva: Mir: 1976).
- B. Liu, J. Ding, J. Yi, J. Yin, *J. Korean Phys. Soc.* **52**, 1483 (2008).